EVALUATION OF INFRASONIC NOISE REDUCTION FILTERS

Michael A. H. Hedlin and Jon Berger

University of California, San Diego

Sponsored by Defense Threat Reduction Agency

Contract No. DTRA01-00-C-0085

ABSTRACT

It is generally accepted that the study of acoustic signals in the atmosphere requires suppression of noise due to atmospheric turbulence. Most acoustic signals of interest arrive with longer spatial wavelengths than the noise that originates near the receiver. As a result, integration of acoustic energy across an area will attenuate spatially de-correlated noise and increase the signal-to-noise ratio. A second approach employs a barrier to reduce wind speeds and small-scale turbulence at the location of the sensor. We are investigating the utility of the various noise-reduction devices that have been proposed or are currently in use. Toward this end, we conduct noise suppression experiments at the Pinon Flat Infrasound test bed in Southern California. This test bed has proved to be ideal for this kind of research as wind speeds vary from near zero to > 15 m/s. The test bed is the site of the 8-element infrasound array IS57 and experiments involving the new fiber optic infrasound sensor. A second goal of our contract is to model the observations and propose remedies for observed shortcomings of the filters.

In our first experiment at Pinon, we tested a wind fence against a 30-m-aperture array of microporous hoses. These data were collected concurrently with unsuppressed noise sampled by a reference port. This test revealed that a 50% porous 2-m wind fence coated with a fine wire mesh reduces infrasonic noise above 0.5 Hz by up to 30 dB. The porous wind fence is not effective at longer periods.

Our second experiment compared the wind fence with an array of 144 open-air ports distributed across an area 70 m in diameter. This is the design favored by the Provisional Technical Secretariat of the Comprehensive Nuclear-Test-Ban Treaty Organization (PTS-CTBTO) for use at locations where wind speeds are commonly above 3 m/s. In this experiment we also compared these filters with an 18-m-aperture multi-port filter (recommended by the PTS for use at relatively calm areas). After > 1 month of recording at wind speeds ranging from near zero to above 15 m/s, we observed significant (15 dB) resonance peaks in the 70-m system at 2.65 and 7.95 Hz. These are the first two eigenfrequencies of an organ-pipe mode inside the nonporous pipes that connect the open ports to the microbarometer. The anti-aliasing filter near 10 Hz removes energy at the higher eigenfrequencies, which are predicted by resonance theory. The peaks become evident at wind speeds below 0.5 m/s. The fundamental resonance peak in the 18-m filter is observed at 9.5 Hz, beyond the band of interest to the monitoring community. Our noise experiment has verified the utility of the 70-m filter for suppression of long-period noise. Noise suppression depends on local wind speeds but will reach 15 to 20 dB between 0.1 and 1.0 Hz. Noise suppression is observed from 50 seconds to above 1 Hz. The 18-m filter is superior to the 70-m filter at frequencies above 0.5 Hz.

How the mechanical noise suppression devices compare with the new fiber optic sensor and with a sensor buried in a shallow porous medium (as proposed by the Southern Methodist University (SMU) group) has not yet been determined.

KEY WORDS: spatial averaging, turbulence, organ-pipe mode

OBJECTIVE

Our objective is to build and test infrasonic noise reduction systems to assess the utility of the different devices as a function of frequency and wind speed. We use chi-squared statistics to assess the significance

of any observed differences in the performance of the different devices. Our goal is to test systems that are being deployed at International Monitoring System (IMS) array sites and to test new devices (such as the new fiber optic sensor under development at UCSD) and spatially compact filters (such as the wind fence, a sensor buried in a porous medium) in our search for systems that are more economical and/or superior to currently preferred designs. We identify shortcomings of filters (e.g. resonance in large pipe filters) and will propose possible remedies.

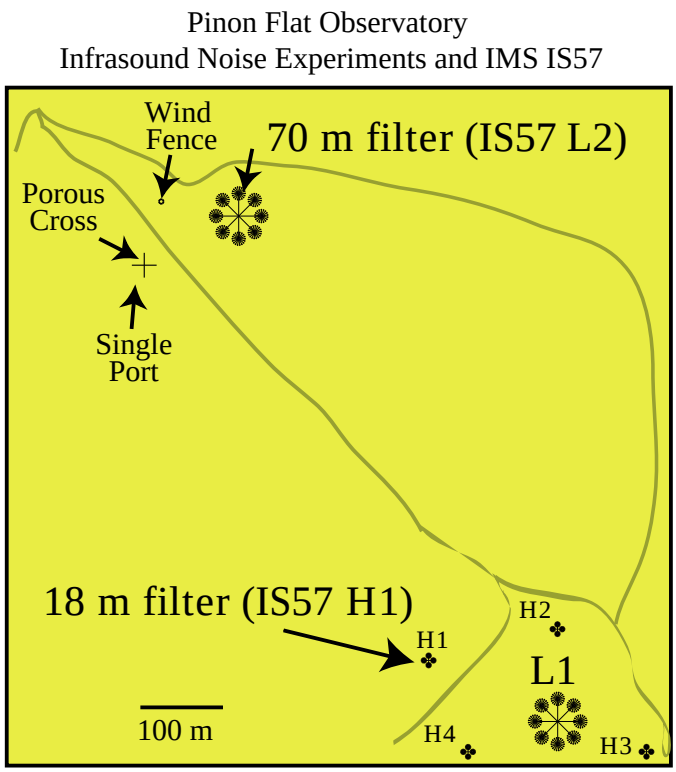

Figure 1. Relative locations of the noise reduction systems at the Pinon Flat Observatory.

RESEARCH ACCOMPLISHED

The Pinon Flat Observatory

All of our experiments have been conducted at the Pinon Flat Observatory (PFO). As an environment for testing the efficacy of the various spatial filters, PFO offers a variety of wide wind conditions. The observatory is located in the Anza Borrego desert ~ 50 km to the southwest of Palm Springs in the coastal ranges. Pinon pine trees and essentially no low-lying ground cover cover much of the area. Wind speeds are often near zero at night and sometimes exceed 15 m/s during the day. Northwest and southeast winds are most common. The observatory is accessible at all times of the year. The International Monitoring System (IMS) infrasound array IS57 is located at PFO (Figure 1). The array comprises 8 instruments distributed across 2km and includes both high-frequency, 18 m, noise reduction systems and low-frequency, 70 m aperture, systems. An IMS auxiliary 3-Component seismic station is located at the NW corner of the observatory. There is essentially no cultural noise in the area.

Noise reduction experiments

For our experiments we used the MB2000 aneroid microbarometer fabricated by the French Departement Analyse et Surveillance de l Environnement (DASE) and now by Tekelec. These sensors provide a filtered signal between 0.01 and 27 Hz (low-passed below 9 Hz by our anti-aliasing filter) with an adjustable sensitivity. We deployed the low sensitivity (20 mV/Pa) version. The electronic noise of the sensor is 2 mPa rms, between 0.02 and 4 Hz, which is well below natural background noise (DASE technical manual, 1998). Each sensor was placed in an insulating case. Each sensor was deployed with ultrasonic wind velocity, air temperature and humidity sensors. The temperature and humidity sensors were located 1 m above the ground. The wind sensor was 2 m above the ground at all sites except within the wind fence. This sensor was located at 1 m, the height of the microbarometer. In all experiments, the infrasound and meteorological signals were digitized at 20 and 1 sps respectively using a 24 bit Reftek 72A-08 data acquisition system. Each system was run on solar power. The experiments were preceded by calibration tests in the field at PFO, and in the laboratory at IGPP in La Jolla, California. The tests were conducted to ensure all field systems were robust and yielded equal digitized signals for equal input.

We have conducted two wind noise experiments since the summer of 2000. For the first experiment, we constructed a 50% porous, 2 m tall, hexagonal wind fence, a 30 m aperture, 4 arm, porous hose filter. Data were also recorded through a single reference port located 5 cm above the ground to indicate the level of

unsuppressed noise at the observatory. The second experiment involved a reference port, a screened wind fence, a 70 m multiport filter and an 18 m multiport filter. The filters are described in greater detail below.

Porous Hose
This simple filter is easy to deploy and, as a result, commonly used to conduct infrasound site surveys. The filter (typically micro-porous garden hose placed on the ground) integrates pressure variations along its entire length. Uncorrelated pressure variations, such as those due to wind turbulence, sum incoherently and are attenuated. Although noise and the signal of interest might have the same time-frequency, the noise, which is most commonly due to wind turbulence, is incoherent over shorter length scales. There are a few, notable, shortcomings of this filter. The signals are integrated with time delays that become significant as the aperture of the filter increases. The microporosity is known to degrade with time with exposure to UV radiation.

The Wind Shelter.
The wind shelter is akin to a forest as it reduces wind speeds inside the shelter and reduces the scale of the atmospheric turbulence so that much of the acoustic energy that results is displaced beyond the frequency band of interest. The design we have chosen to test has been used by Ludwik Liszka at the Swedish Institute of Space Physics and was forwarded to us by Doug Revelle (LANL). Our fence is shown in Figure 2. The design features of a fence (including the shelter height and porosity) are dependent on conditions at the site (Doug Revelle, personal communication). For example, the height of the shelter is dependent on the roughness of the surrounding topography and local mean wind speeds. A wind speed experiment we conducted at the observatory, in which we collected wind velocity at 1.0, 2.0 and 5.0 m, indicates that a 2 m tall fence is appropriate for this site. In our first two experiments, we tested a wind fence that had 50% porosity with and without an additional wire mesh. In our upcoming experiment, we will test a wind fence that has 0% porosity on the sides and is covered by a wire mesh. In all experiments, the sensor in the wind fence is enclosed in foam inside a porous aluminum shell.

Multiport filters
A new design which employs discrete low-impedance ports was conceived by Benoit Alcoverro at the Departement d'Analyse et de Surveillance de l'Environnement (DASE). This space filter distributes low-impedance ports spatially and signals are summed at a central manifold after propagation through impermeable pipes. The key features of this design is that the propagation distance, and thus the time delay, from each port to the summing manifold is equal and thus phase delays are eliminated. The impedances between the ports and the primary summing manifold are the same for all ports. Doug Christie (PTS, CTBTO) has proposed several innovative space filters based on this idea. The space filters range from 92 ports distributed over an area 18 m across to 144 ports covering an area 70 m across (Figure 2). The smaller filter is considered to be effective at high frequencies. The 70 m aperture filter is considered appropriate for windy sites that require long-period noise suppression.

The aim of all mechanical filters is to sample the atmosphere at a series of points and add their pressure signals mechanically by joining many tubes to a single microbarograph. Because of the finite sound velocity, there are phase delays along the lengths of the pipes, limiting the area that can be averaged over with mechanical filters. Further, because of the size of these spatial filters there is no practical way of measuring their response.

An Optical Fiber Sensor.
Work on an entirely new kind of infrasound sensor - an Optical Fiber Infrasound Sensor (OFIS)- is now underway at IGPP. The OFIS consists of a long optical fiber whose optical path length is sensitive to the ambient atmospheric pressure. The OFIS integrates pressure variations that occur along the line in space defined by the optical fiber s path. The averaging characteristics are governed by the speed of light, so we can make the line over which pressure is averaged extremely long (many km). The distributed sensor approach has many advantages.

In this paper, we will focus on the second experiment. A test of the fibre optic sensor is planned for the

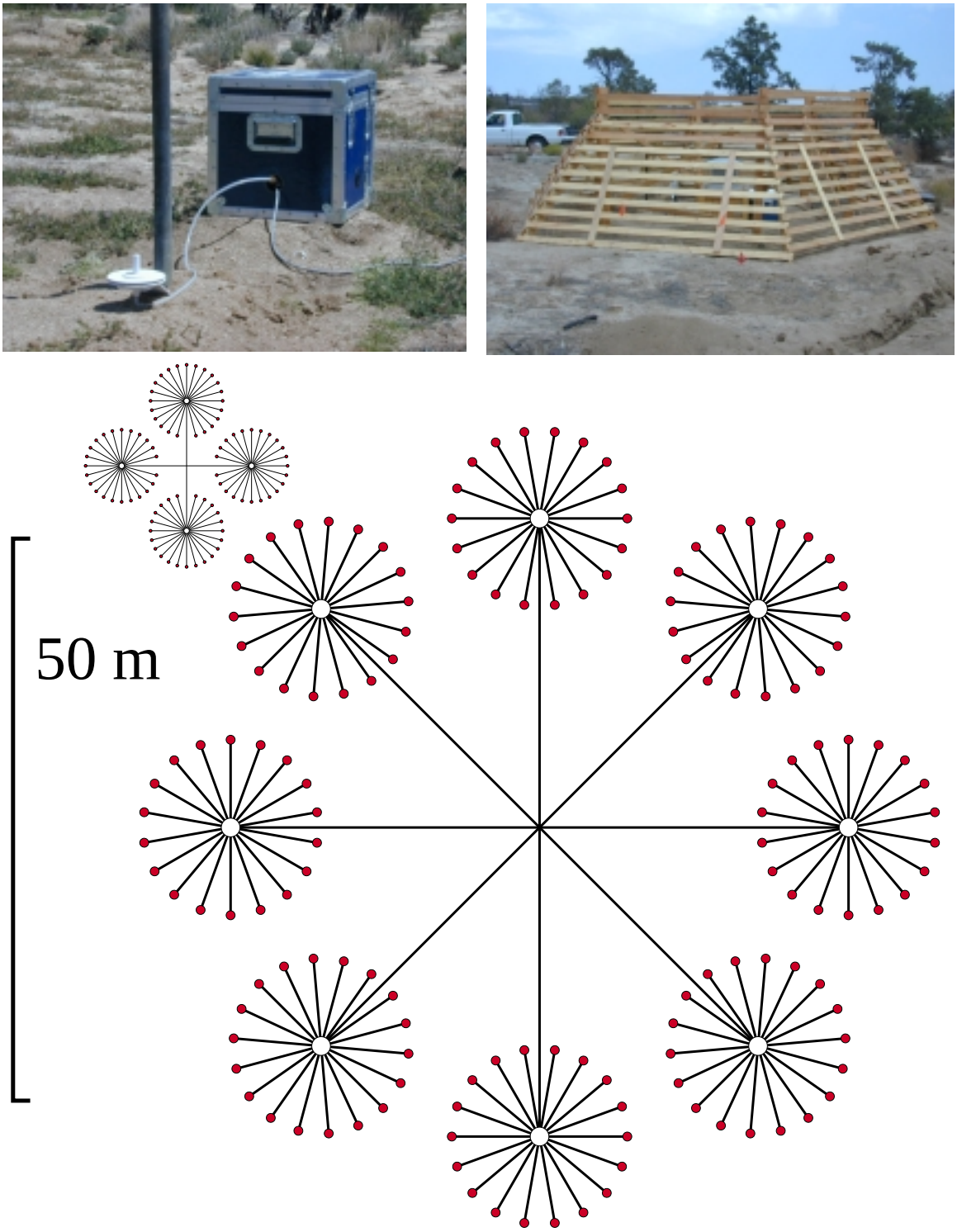

Figure 2. The reference port (upper left), the unscreened 50% porous wind fence (upper right), the 18 m multiport filter and 70 m filter were tested at PFO. In two separate experiments, we tested the wind fence as shown above and coated with a fine wire mesh. The 18 m diameter noise-reducing pipe array is recommended by the Provisional Technical Secretariat for use at high-frequency IMS array elements at stations located in higher wind areas or at all array elements at stations located in low wind areas. The 70 m diameter filter is recommended for use at low-frequency elements in high wind speed areas. The 18 m filter has 92 open-air ports, the 70 m filter has 144 ports.

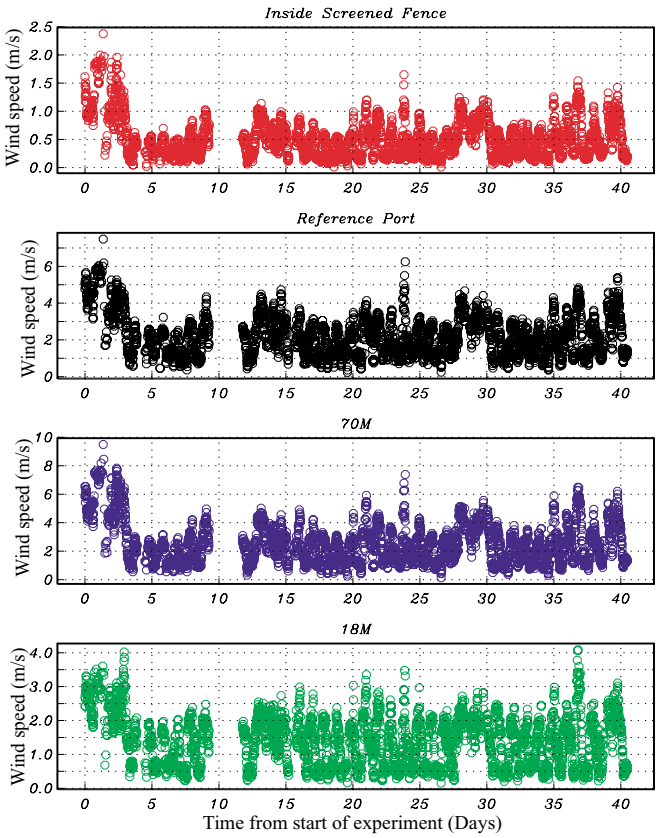

Figure 3. 15 minute average wind speeds taken every 15 minutes during the experiment. Ultrasonic wind sensors were located at 1 m elevation inside the wind fence and at 2 m at the other sites.The data were telemetered in real time to our lab in La Jolla. The break in coverage around day 10 of the experiment resulted from a temporary break in this link.

summer of 2001.

Wind Speed

An essential component of any noise reduction experiment is wind speed data. In Figure 3 we plot wind speeds collected during the main, second, experiment averaged over 15 minute time intervals. Instantaneous wind speeds outside the wind fence occasionally exceed 15 m/s. Diurnal variations are evident at all sites. Wind speeds are lowest in the wind fence and at the site of the 18 m filter, which was located in a sparse Pinon pine forest. We have observed that the screened wind fence reduces wind speeds by up to 90%.

Stacked Spectra

At the heart of our analyis of recorded data is the calculation and stacking of power spectral estimates. Stacking is necessary to reduce the statistical uncertainty inherent in the spectral estimation process and clearly reveal the dependence of average noise levels on wind speeds. We divide the filtered pressure records at each site into 15 minute intervals. The second experiment spanned > 768 hours and thus yielded 3074 time intervals. From each 15 minute segment of data, we calculate a Welch time-averaged power spectrum. Although we collected wind speed data at all sites, for the purpose of comparing data collected at the same time at the different sites, we used just the wind speed data collected at 2 m at the reference port. The wind speeds in the wind fence were reduced sharply by the walls of the fence. The wind speeds at the 18 m element were also reduced by the forest (Figure 3). To describe the increase of infrasonic noise at the different sites with increasing wind speed, we bin the spectral estimates into 0.5 m/s wind speed intervals. The result is shown in Figure 4. In this figure, each curve in each panel represents a single bin. The lowest curve in each panel corresponds to estimates taken when the wind at the reference site was < 0.5 m/s. At the four sites, we see infrasonic noise increases at all frequencies with increasing wind speed. The microbarom peak is most clearly resolved at the 70 m filter. The peak is seen clearly at wind speeds up to 1.5 m/s and in some individual spectra at wind speeds up to 2.5 m/s. The effectiveness of this filter at reducing infrasonic noise below 1 Hz is evident however the resonance peaks above 1 Hz are significant at all wind speeds (Figures 5 and 6). We observe peaks at 2.65 and 7.95 Hz. The frequency of the second resonance peak is 3.0042 times the first (Figure 5). The frequencies of the two observed peaks are nearly independent of wind speed (Figure 5) and temperature. From 0 to 35°C, the frequency of the first peak rises 1.5%, the second rises 0.8%. The pipes in this filter were buried ~ 0.60 m. The temperature was measured 1 m above the surface. The resonance peaks depend on the acoustic velocity in the pipes, which depends strongly on the temperature. The independence of the resonant frequency on temperature indicates the level of insulation provided by the ground. The separation between the resonance peaks is equal to 1/T, where T is the travel time between reverberations. This equals V/L, where V is the acoustic velocity and L is the distance. From 0 to 35°C, the separation in the resonance peaks is estimated to change from 5.2924 to 5.3064 Hz. As

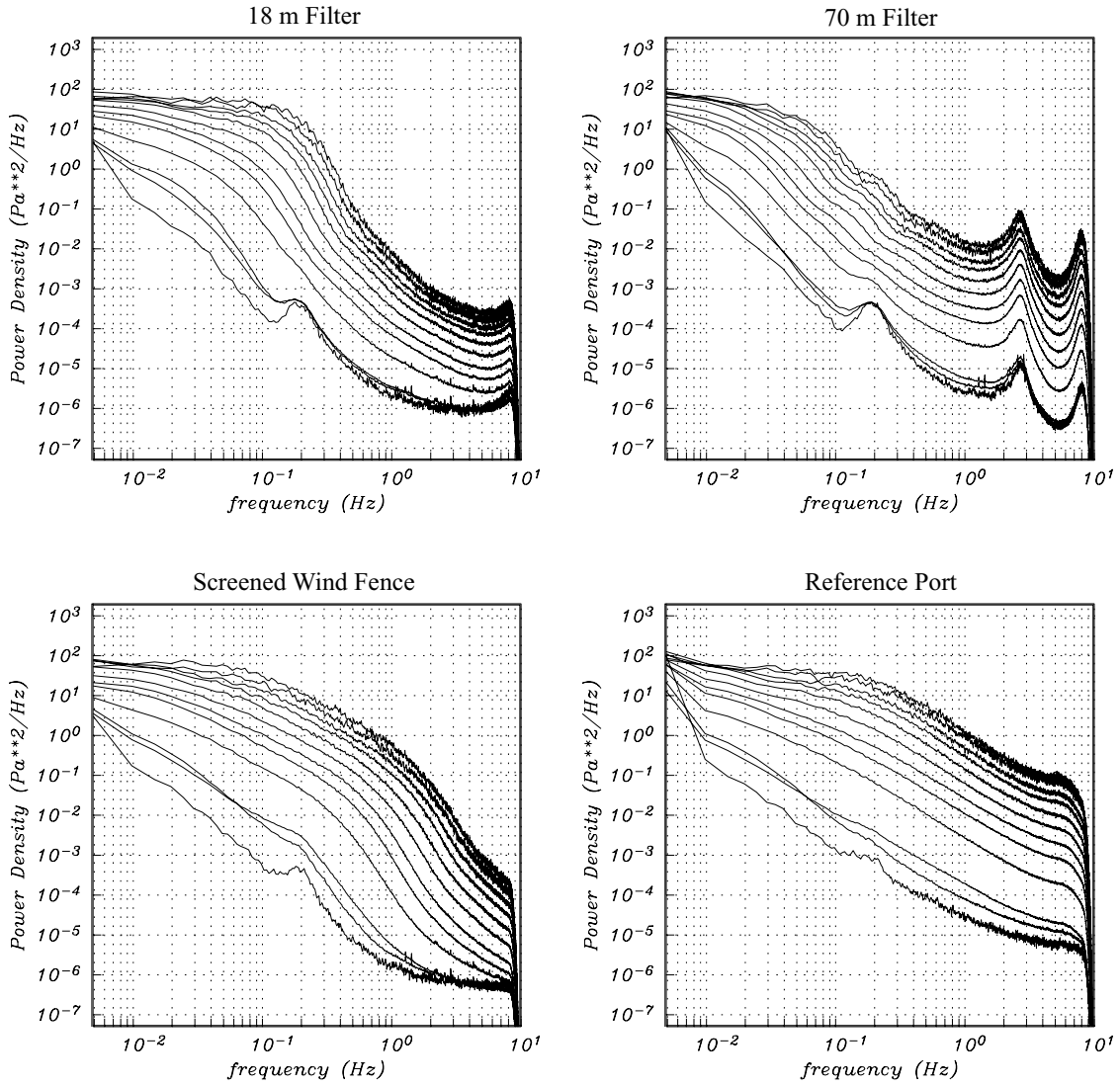

Figure 4. Average power spectra as a function of wind speed. Each curve represents the average power density determined from an unweighted stack of individual power spectral estimates. Estimates were binned by wind speed measured at a height of 2 m at the reference site. Each bin spanned 0.5 m/s in speed, with the first bin beginning at 0.0 m/s.. Power spectral estimates were taken from 15 minute intervals of data.The microbarom peak is seen most clearly at the 18 and 70 m filters at wind speeds below 1.5 m/s. Infrasonic power at all four sites rises rapidly between 1.5 and 2.0 m/s. Resonance peaks are seen in the data from the 70 m filter at ~ 2.67 and 7.95 Hz.In total, there were 3074 spectral estimates from 768.5 hours of recording. The bin from 1.0 to 1.5 m/s included > 800 spectral estimates.

L is unchanged, the frequency change implies a velocity change of 0.26%. As the acoustic velocity (in dry air) is ~ 20.07 (K)^0.5 (McKisic, 1997), where K is temperature in °K, this indicates that the temperature varied in the pipe by 1.4°C, well below the temperature variation at 1 m of 35°C.

Modeling Resonance in the multiport filters

Resonance enriches the spectrum at certain, equipspaced, frequencies and produces substantial coda. Following Sereno and Orcutt (1985), who observed resonance in recordings of seismic energy that propagates in the oceanic water column and sediment, we model resonance in multiport pipe systems as follows. We consider a wavelet, w(t), resonating in a simplified pipe system that consists of a single pipe, open at

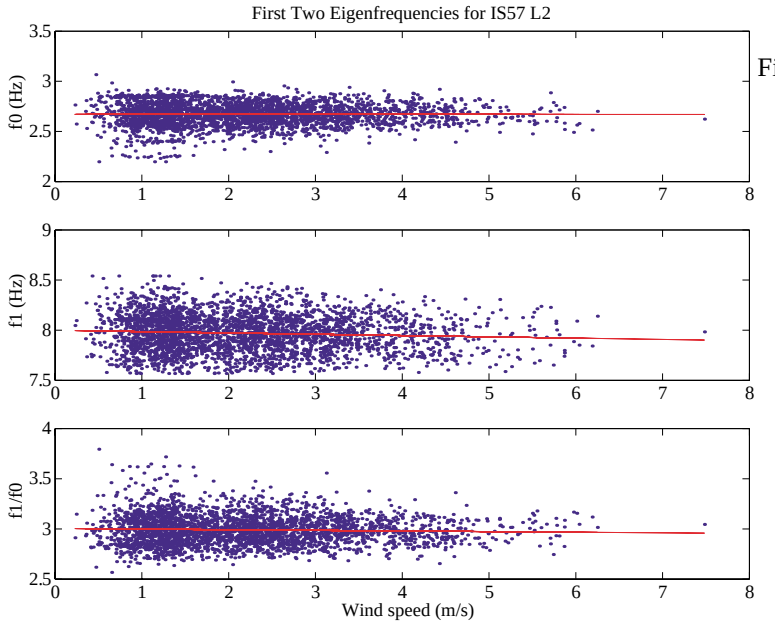

Figure 5. Resonance peaks in data from the 70 m filter at IS57 L2 as a function of wind speed. Only a very weak dependence on wind speed is observed. The linear fit indicates that the first peak, f0, is given by .0001V + 2.6701 (where V is wind velocity). f1 = 0.013V+7.9985. The ratio of the two peaks is 3.0042. The dependence on temperature, T, is f0 = 0.0013T+2.643; f1 = 0.0017T+7.9354 where T is temperature in °C.

both ends. The linear sum of all reverberations at the half-way point of the pipe (where the microbarometer is located) is given by:

$$x(t) = w(t) * \left[\tfrac{1}{T} III\ (\tfrac{t}{T})\ e^{-\alpha|t|} H(t) e^{-i\pi \frac{t}{T}} \right]$$

where T is the time between successive reverberations and is equal to L/V where L is the length of the pipe and V is the acoustic velocity in the pipe. The shah function is tapered exponentially to simulate the effect of attenuation due to propagation in the pipe and leakage at the reflection points. The Heaviside step function, H(t), excludes any acausal energy. The final exponential is required by the p phase shift incurred by reflection at each end of the pipe. By Fourier transforming this equation, we see that the spectrum of the original wavelet is multiplied by an infinite set of staggered tapering functions which decay at a rate determined by the attenuation parameter a. The amplitude spectrum of the sum of wavelets is given by:

$$|\tilde{X}(f)| = |\tilde{W}(f)||III(fT + \tfrac{1}{2}) * \ \tfrac{\alpha - i2\pi f}{(\alpha^2 + 4\pi^2 f^2)}\ |$$

The theory predicts spectral modulations at $f_n = (2n+1)/(2T)$ - the eigenfrequencies of an organ-pipe mode (Aki and Richards, 1980). The longer the pipe, or equivalently the slower the acoustic wave propagation in the pipe, the more closely spaced the spectral highs will be. In the 70 m filter, the first and second resonance peaks are predicted, and observed, at 2.67 and 7.95 Hz respectively (Figure 5). Without the phase shift at the reflection points, the second spectral peak would be observed at double, not triple, the frequency of the first. Using the recording from the single reference port as the basic wavelet, we find that the spectral peaks observed in the 70 m filter are accurately reproduced by this simple theory (Figure 7). We are preparing a more complete theory that describes resonance in the full pipe system shown in Figure 2 and uses attenuation and acoustic velocity parameters constrained more accurately by observation.

Comparison of different noise reduction systems

Figure 8 summarizes the intercomparison of the 18 and 70 m multiport filters with the screened wind fence and the reference port. The 12 panels show the binned and averaged spectral estimates from all four sites and the 95% confidence limits from a chi-squared analysis at wind speeds ranging from 0 to 0.5 m/s (first panel) to 5.5 to 6.0 m/s (lower right panel). We observe the growth of infrasonic noise at all sites with

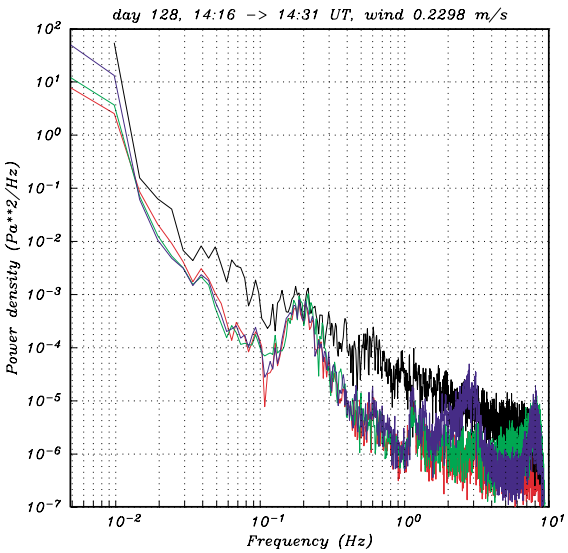

Figure 6. Power spectral estimates taken from the 4 filters at the lowest wind speed observed during the experiment. The resonance peaks in the data from the 70 m filter (blue curve) are clearly observed at a time when wind speeds average 0.23 m/s.

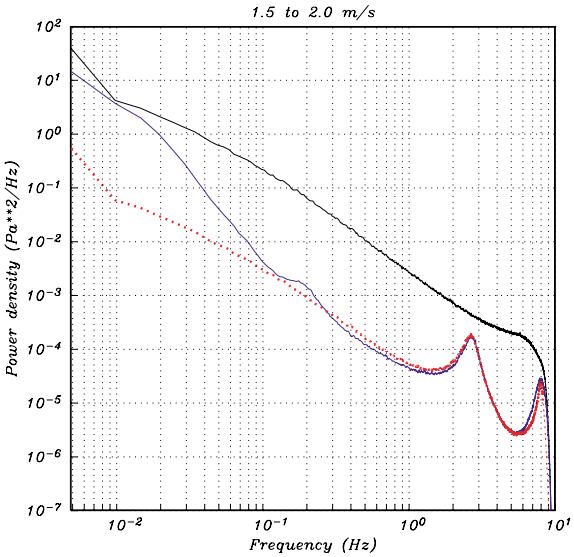

Figure 7. Linear superposition theory accurately reproduces the resonance peaks. In this figure, we show the average spectral estimate from the reference port (black), and the 70 m filter (blue) for the bin between 1.5 to 2.0 m/s. The simulation is shown in red.

increasing wind speed. The confidence limits are broadest at the highest and lowest speeds as we have relatively few spectral estimates in those bins. The bin from 1.5 to 2.0 m/s represents stacks of > 800 spectral estimates. At this wind speed, the confidence limits are indistinguishable from the averages. We observe statistically significant differences in the noise levels between all sites at all wind speeds. All filters reduce noise levels except at the longest periods. Presumably, noise reduction at periods above 50 s is beyond any practical mechanical noise reduction scheme. The 70 m filter provides the most significant noise reduction at long periods. The microbarom peak is not seen in the recordings made via the reference port or in the wind fence except at the lowest wind speeds (Figures 6 and 8).

Signals from the April 23 meteor explosion

The widely reported explosion of a large meteor west of Baja California on April 23, 2001 was recorded by the IMS array IS57 and by all sites in our noise experiment. The large signals provide an opportunity for us to determine the extent, if any, to which signal is degraded by the different filters. Preliminary results are shown in Figure 9. The timeseries from the 18 and 70 m filters are indistinguishably eye from the one obtained via the reference port. The latter, presumably, gives the truest representation of a signal that is significantly above noise. The power spectral estimates, however, show the extent to which resonance distorts the high frequency end of the signal spectrum.

CONCLUSIONS AND RECOMMENDATIONS

Planned wind noise experiments

Our third noise reduction experiment will occur during the summer of 2001. We will test a wind fence that has solid walls, and a screen across the top, against the fibre optic sensor. We will also bury a sensor in a fine gravel pit following specifications developed by the SMU group. Two sites at the IMS array use 70 m filters that are located in insulating pipes at the surface. We will test one of these filters to assess the effectiveness of the insulation at moderating temperature variations in the pipes and reducing convective

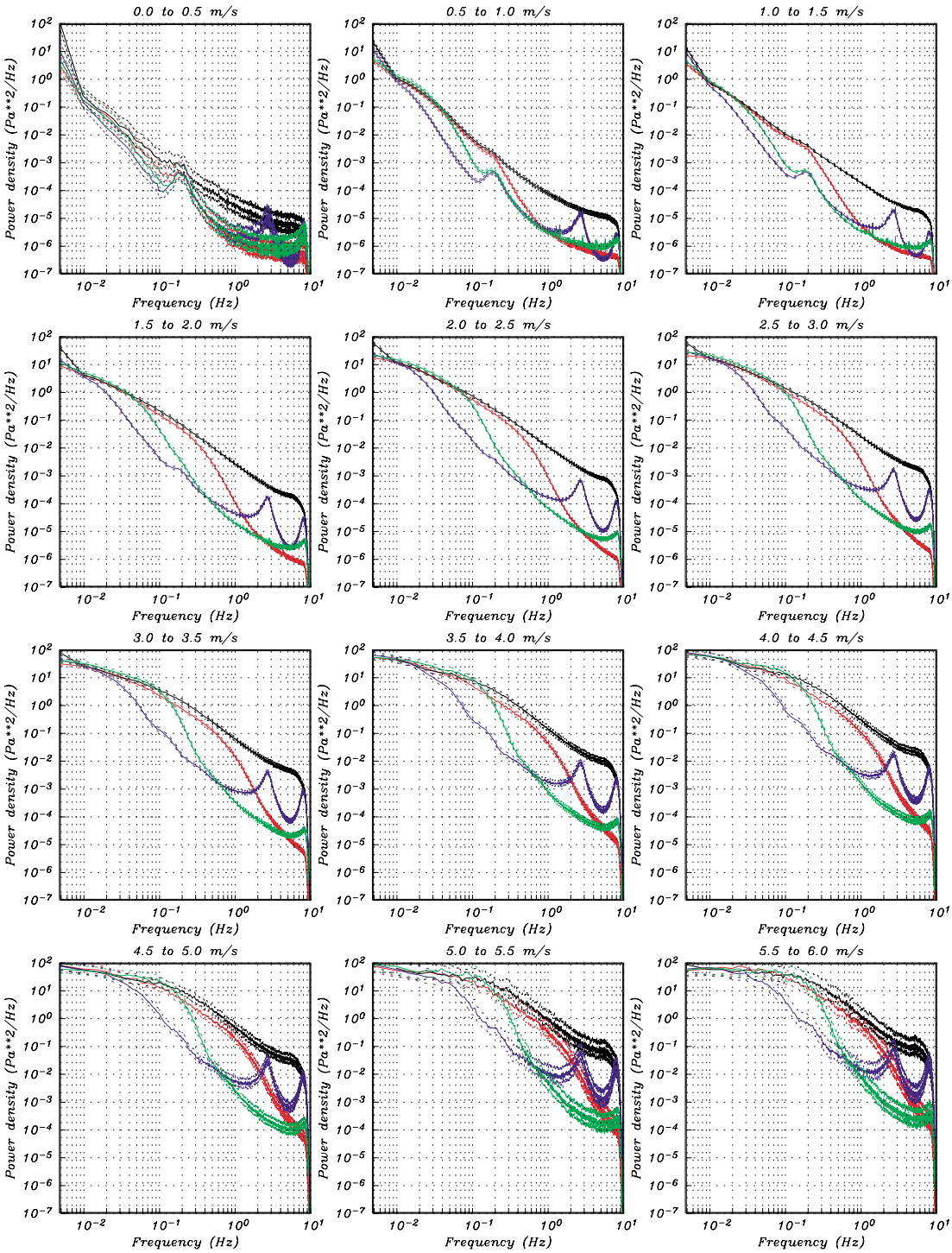

Figure 8. Average power spectral estimates taken from noise recordings at the reference port (black), the screened wind fence (red), the 18 m multiport filter (green) and the 70 m filter (blue). Wind speeds were taken at 2 m at the reference site and averaged over 15 minutes. Plotted with the average spectral estimates are 95% chi-squared confidence limits. The limit curves are indistinguishable from the averages at wind speeds between 2 and 5 m/s. At low and high wind speeds, the coverage is low and the uncertainty is relatively large. The resonance peaks in the 70 m filter are seen to be significant at all wind speeds however this filter is highly effective at long periods. No filter suppressed noise at periods beyond 50 s to 100 s.

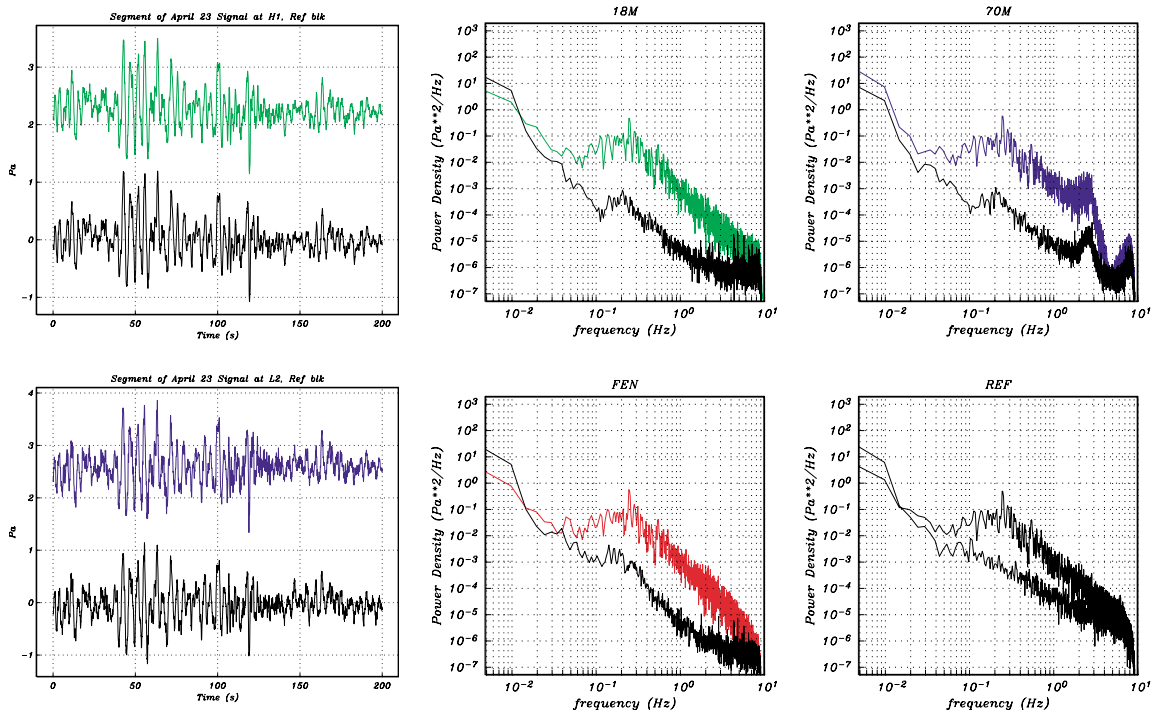

Figure 9. The widely reported explosion of a large meteor off the coast of California was recorded by the IMS array IS57 at PFO and by sensors in our wind noise experiment. On the left, we show recordings from the reference port (black) and from the 18 m filter (green-top) and 70 m filter (blue). Spectral estimates from the four sites are shown to the right. The 18 m filter, 70 m filter, wind fence and reference port are shown to the right in the upper left, upper right and lower two panels respectively.

noise in the acoustic pipes.

The resonance problem

We are considering a number of solutions to the resonance problem observed in the 70 m filter. The first step in our analysis of this problem is modeling the reverberations. Our first attempt at modeling the resonance peaks was presented in this paper. We will now extend this theory to cover resonance in a pipe filter with an arbitrary number of arms (8 are used in the 70 m filter) and secondary resonance in the clusters of shorter pipes. The primary and secondary pipes produce separate sets of resonance peaks. The theory will allow us to experiment with any combination of secondary and primary pipe lengths. We will seek designs in which resonances are less significant. We will also explore mechanical changes to the port design that might limit the amplitude of the reflections.

We will transmit controlled signals in pipes to measure the phase shift at the reflection points and the attenuation of the signal with time as well as the acoustic velocity.

REFERENCES

Aki, K., and P.G. Richards (1980), Quantitative Seismology: Theory and Methods, W.H. Freeman, San Francisco, Calif.

McKisik, J.M. (1997), Infrasound and the infrasonic monitoring of atmospheric nuclear explosions: A literature review, Final report submitted to the DOE and Phillips Lab, PL-TR-97-2123.

Sereno, T.J., and J.A. Orcutt (1985), Synthesis of realistic oceanic Pn wave trains, *J. Geophys. Res.*, 90, 12755-12776.